Hydrodynamic behavior of lattice Boltzmann and lattice Bhatnagar-Gross-Krook models

O. Behrend and R. Harris*
Department of Physics, The University of Edinburgh, Mayfield Road, Edinburgh EH9 3JZ, United Kingdom

P. B. Warren
Unilever Research, Port Sunlight Laboratory, Quarry Road East, Bebington, Wirral L63 3JW, United Kingdom
(Received 20 June 1994)

We present a numerical analysis of the ranges of validity of classical and generalized hydrodynamics for lattice Boltzmann and lattice Bhatnagar-Gross-Krook (BGK) methods in two and three dimensions, as a function of the collision parameters of these models. Our analysis is based on the wave-number dependence of the evolution operator. Good ranges of validity are found as long as the BGK relaxation time is chosen smaller than or equal to unity. The additional degree of freedom in a two parameter BGK model can give further improvements.

PACS number(s): 05.20.Dd, 05.50.+q, 05.60.+w

I. INTRODUCTION

Recently, lattice gas automata (LGA) methods have been developed as a new computational approach to fluid dynamics [1–3]. Using purely local Boolean operations to represent particle collisions, they have proved to be extremely efficient, although, due to the fluctuations inherent in the method, statistical averaging is necessary in order to extract information. The lattice Boltzmann (LB) method [4–6] and the lattice Bhatnagar-Gross-Krook (BGK) method [7–10], by using continuous distribution functions, eliminate this statistical noise and offer significant computational advantages.

When the LB method was first introduced [4], a collision operator was constructed directly from the collision rules of the underlying LGA. It was soon realized, however, that the collision operator could be linearized about an equilibrium distribution function and replaced by a collision matrix [5,6]. Furthermore, it was realized that the collision matrix and equilibrium distribution function need not be constrained to follow the original LGA and there was in fact a great deal of freedom in the choice of these entities [10–13].

It is important to define ways in which these choices can optimize the behavior of the models. In the past one of the main applications has been the study of flows at high Reynolds number and it has been customary to minimize the viscosity by tuning the parameters of the collision operators. However, since applications to low Reynolds number flows are becoming increasingly important [14,15], other criteria become relevant.

For specific applications, of course, there are always particular ways to improve numerical stability and reproducibility, but in all cases it is important to define the spatial scale for which the models reproduce hydrodynamics and to investigate how this scale depends upon the parameters of the simulation. Without such information, it is difficult to give unambiguous interpretations of the numerical data [16].

In the literature, this approach is well known from the application of the **k**-dependent Boltzmann equation to continuous fluids [17]. For lattice gases, the analysis was first considered in detail by Luo *et al.* [18] and developed by Grosfils *et al.* [19] and Das, Bussemaker, and Ernst [16] for the study of LGA's. The latter authors show that some of the simplest LGA models reproduce classical or even generalized hydrodynamics only over very large spatial scales and point out that observations in the literature of "negative viscosities" [20] can be traced to this restricted regime of applicability. The **k**-dependent analysis of the LB method has also been used by various authors [5,13,12] to help understand the limits of validity of the new method. We present in this paper a full analysis of the validity of hydrodynamics for the commonly used models in two and three dimensions, using the **k**-dependent wave-vector approach.

In Sec. II we consider in detail the specification of the models and concepts related to the LB method. We characterize the collision matrix by its eigenvectors and eigenvalues so that we can study the original LB method, the BGK method, and possible generalizations using a common formalism. In Sec. III we set up the wave-vector formulation and in Sec. IV consider some results for general models. We consider the unit relaxation time model separately in Sec. V since it is a special case. Finally, in Sec. VI we draw conclusions on the ranges of validity of the models and discuss related factors.

II. SPECIFICATION OF THE MODELS

In a typical LB model a set of nodes form a regular d-dimensional lattice. Each node is connected to other nodes in its local neighborhood by a set of n links, there

*Permanent address: Department of Physics and Centre for the Physics of Materials, McGill University, Rutherford Building, 3600 University Street, Montréal, Québec, Canada H3A 2T8.

being an identical set of links for each node. To denote a typical model we use the symbol DdQn, following the notation of Qian, d'Humières, and Lallemand [9], to mean an n-link model on a d-dimensional lattice.

An occupation number $f_i(\mathbf{r},t)$ is associated with link i of node $\mathbf{r}$ at time t. The occupation numbers undergo collisions at the nodes, where the behavior is determined by the collision matrix and the equilibrium distribution function, and then propagate along the links to the neighboring nodes, where the process repeats. Each cycle of collision and propagation constitutes a time step. Thus the occupation numbers obey the kinetic equation [13]

$$f_i(\mathbf{r}+\mathbf{c}_i,t+1)=f_i(\mathbf{r},t)+\sum_j w_j C_{ij}[f_j(\mathbf{r},t)-f_j^{(\mathrm{eq})}(\mathbf{r},t)] , \tag{1}$$

where C_{ij} is a linearized collision matrix and $f_i^{(\mathrm{eq})}(\mathbf{r},t)$ is an equilibrium distribution function. The sum is over the set of links j connected to the node: w_j is a weight associated with link j.

As well as connecting nodes on a regular lattice, the links must be chosen to achieve isotropy of tensors up to fourth rank formed from sums over the set. Denoting the magnitude and direction of the ith link by a vector $\mathbf{c}_i$, they must satisfy

$$\begin{aligned}
&\sum_i w_i=b, \quad \sum_i w_i c_{i\alpha}=0 , \\
&\sum_i w_i c_{i\alpha}c_{i\beta}=\frac{bc^2}{D}\delta_{\alpha\beta}, \quad \sum_i w_i c_{i\alpha}c_{i\beta}c_{i\gamma}=0 , \\
&\sum_i w_i c_{i\alpha}c_{i\beta}c_{i\gamma}c_{i\delta}=\frac{bc^4}{D(D+2)}[\delta_{\alpha\beta}\delta_{\gamma\delta}+\delta_{\alpha\gamma}\delta_{\beta\delta}+\delta_{\alpha\delta}\delta_{\beta\gamma}] ,
\end{aligned} \tag{2}$$

where greek subscripts α, β, etc. denote spatial indices; the $\delta_{\alpha\beta}$, etc. are conventional Kronecker delta functions; and b, D, and c^2 are parameters. These parameters must be regarded as being defined by Eqs. (2), although the notation has derived from the LGA. Note that the parameter D is not necessarily the same as the space dimension of the lattice d. Specific details of the lattices and links for several common models are given in the Appendix.

The weight w_i appears in nearly all sums over i and we introduce the extension in notation proposed by Vergassola, Benzi, and Succi [12] in which we regard A_i, B_i, etc. as components of *link vectors* $\mathbf{A}$, $\mathbf{B}$, etc., which lie in an n-dimensional *link-vector space*. A generalized dot product

$$\mathbf{A}\circ\mathbf{B}\equiv\sum_i w_i A_i B_i \tag{3}$$

is then defined. The collision matrix can likewise be regarded as a linear collision operator $\mathbf{C}$, which acts on link vectors. We shall also have occasion to use the conventional spatial dot product, which we denote $\mathbf{x}\cdot\mathbf{y}$ or $x_\alpha y_\alpha$. Summation convention will be used with spatial indices α, β, etc., but not with link indices i, j, etc.

In a typical LB equation the linear collision operator can be characterized by its eigenvectors and eigenvalues as follows [12]. The matrix has one so-called density mode eigenvector, d momentum mode eigenvectors, $d(d+1)/2$ stress mode eigenvectors, and a number of ghost mode eigenvectors which span the remaining link-vector space. We denote these eigenvectors by $\mathbf{A}^\rho$, $\mathbf{A}^{\mathbf{J}}$, $\mathbf{A}^S$, and $\mathbf{A}^G$, respectively (so that $\mathbf{A}^{\mathbf{J}}$, for example, represents both the individual eigenvectors and the set of eigenvectors depending on the context). Normalized density and momentum mode eigenvectors are given explicitly by

$$A_i^\rho=\frac{1}{\sqrt{b}}1_i, \quad A_i^{\mathbf{J}}=\left[\frac{D}{bc^2}\right]^{1/2}c_{i\alpha} . \tag{4}$$

The stress mode eigenvectors may be constructed from the $d(d+1)/2$ linearly independent components of

$$Q_{i\alpha\beta}=c_{i\alpha}c_{i\beta}-c^2/D\delta_{\alpha\beta} \tag{5}$$

via a Gram-Schmidt orthogonalization procedure for example [21]. The ghost mode eigenvectors are model dependent and we will not need explicit expressions for them.

The reason for the names of the eigenvectors is that they project out the relevant quantities when they act on the occupation number link vector $\mathbf{f}$ at any particular node. Thus

$$\begin{aligned}
&\rho=\sum_i w_i f_i\sim\mathbf{A}^\rho\circ\mathbf{f}, \quad J_\alpha=\sum_i w_i f_i c_{i\alpha}\sim\mathbf{A}^{\mathbf{J}}\circ\mathbf{f} , \\
&S_{\alpha\beta}=\sum_i w_i f_i Q_{i\alpha\beta}\sim\mathbf{A}^S\circ\mathbf{f} ,
\end{aligned} \tag{6}$$

where ρ, $\mathbf{J}$, and S are the density, the momentum, and the stress in the fluid at the node in question.

The eigenvectors form a complete set in the sense that

$$\sum_{x=\rho,\mathbf{J},S,G} A_i^x A_j^x=\frac{\delta_{ij}}{w_i}\equiv I_{ij} . \tag{7}$$

The sum is taken over the complete set of density, momentum, stress, and ghost mode eigenvectors in an obvious extension of notation. We have defined a generalized identity operator I appropriate to the generalized dot product introduced above.

To facilitate later arguments we construct projection operators such as

$$\begin{aligned}
&P_{ij}^{\rho\mathbf{J}}=\sum_{x=\rho,\mathbf{J}} A_i^x A_j^x=\frac{1}{b}+\frac{D}{bc^2}\mathbf{c}_i\cdot\mathbf{c}_j , \\
&P_{ij}^{SG}=\sum_{x=S,G} A_i^x A_j^x=\frac{\delta_{ij}}{w_i}-\frac{1}{b}-\frac{D}{bc^2}\mathbf{c}_i\cdot\mathbf{c}_j .
\end{aligned} \tag{8}$$

Thus $\mathbf{P}^{\rho\mathbf{J}}$ projects vectors onto that part of the link-vector space spanned by the density and momentum mode eigenvectors of the linear collision operator, and so on. Other projection operators such as $\mathbf{P}^\rho$, etc. can likewise be defined.

Now let us apply the formalism developed above to a discussion of the kinetic equation (1). First, we consider the equilibrium distribution function. This is chosen so that the Navier-Stokes equations are recovered correctly in a multiscale expansion [10]. In general $f_i^{(\mathrm{eq})}$ involves nonlinear terms in the mean velocity of the lattice gas, but in a linear analysis we may drop these terms and just

consider [10]

$$f_i^{(\mathrm{eq})}=\frac{\rho}{b}+\frac{D}{bc^2}\mathbf{J}\cdot\mathbf{c}_i\ , \tag{9}$$

where ρ and $\mathbf{J}$ are the density and the momentum of the fluid at the node in question (it can also be shown that this equilibrium distribution function gives rise to the Stokes, or creeping flow, equations). As already suggested by Eq. (6), the equilibrium distribution function can also be written as

$$\mathbf{f}^{(\mathrm{eq})}=\mathbf{P}^{\rho\mathbf{J}}\circ\mathbf{f} \tag{10}$$

using the generalized dot product notation and the projection operator introduced above. Inserting this expression in the kinetic equation (1) shows that one may write

$$f_i(\mathbf{r}+\mathbf{c}_i,t+1)=f_i(\mathbf{r},t)+\sum_j w_j C_{ij}^R f_j(\mathbf{r},t)\ , \tag{11}$$

where a *right-projected* collision matrix $\mathbf{C}^R=\mathbf{C}\circ\mathbf{P}^{SG}$ has been introduced, the projection operator having been defined in Eq. (8).

This analysis now allows us to consider the original LB model, the BGK model, and possible generalization using a unified approach. First, in the original LB model derived from the LGA [5], the linearized collision matrix conserves particle number and momentum; thus the density and momentum mode eigenvectors have eigenvalue zero. The stress mode eigenvectors are degenerate with eigenvalue λ and the ghost mode eigenvectors may be wholly or partially degenerate, having one or two eigenvalues depending on the model in question. Given that $\mathbf{A}^\rho$ and $\mathbf{A}^\mathbf{J}$ are eigenvectors with zero eigenvalue it is apparent that, in this case, $\mathbf{C}^R$ is identically equal to $\mathbf{C}$.

In the single relaxation time or BGK method [8,9], the collision matrix is $\mathbf{C}=-\mathbf{I}/\tau$ so that all the f_i relax towards $f_i^{(\mathrm{eq})}$ by the same factor at each time step (τ plays the role of a relaxation time). The right-projected collision matrix is given by $\mathbf{C}^R=-\mathbf{P}^{SG}/\tau$. It is clear that $\mathbf{C}^R$ has density and momentum mode eigenvectors again with eigenvalue zero and stress and ghost mode eigenvectors with a common eigenvalue $\lambda=-1/\tau$.

We can also consider a two-parameter model, slightly more general than the BGK model, in which we allow separate relaxation parameters for the stress and ghost modes. We set $\mathbf{C}^R=\lambda\mathbf{P}^S+\sigma\mathbf{P}^G$, where σ is the common eigenvalue of the ghost mode eigenvectors. Explicitly

$$C_{ij}^R=\sigma\left[\frac{\delta_{ij}}{w_i}-\frac{1}{b}-\frac{D}{bc^2}\mathbf{c}_i\cdot\mathbf{c}_j\right]+(\lambda-\sigma)\sum_{x=S}A_i^x A_j^x \tag{12}$$

since $\mathbf{P}^G=\mathbf{I}-\mathbf{P}^S-\mathbf{P}^{\rho\mathbf{J}}$ and $P_{ij}^S=\sum_{x=S}A_i^x A_j^x$. This two-parameter BGK model is the same as the original models derived from the LGA, when the ghost mode eigenvectors are fully degenerate in the latter. It reduces to the conventional BGK model when $\lambda=\sigma=-1/\tau$.

Linear stability analysis requires all eigenvalues to lie in the interval $(-2,0)$ [13]. Additionally the kinematic viscosity is explicitly determined by the stress eigenvalue via [13]

$$\nu=-\frac{c^2}{(D+2)}\left[\frac{1}{\lambda}+\frac{1}{2}\right]\ . \tag{13}$$

Note that $\nu>0$ also requires $\lambda\in(-2,0)$.

III. WAVE-VECTOR FORMULATION

To analyze the hydrodynamic behavior of these models we introduce an evolution operator $\mathbf{H}(\mathbf{k})$ defined by Fourier transforming the kinetic equation (11) such that

$$f_i(\mathbf{k},t+1)=\sum_j w_j H_{ij}(\mathbf{k})f_j(\mathbf{k},t)\ . \tag{14}$$

In terms of the right-projected collision matrix introduced above, $\mathbf{H}(\mathbf{k})=\mathbf{D}(\mathbf{k})\cdot(\mathbf{I}+\mathbf{C}^R)$, where $\mathbf{D}(\mathbf{k})$ is a diagonal displacement operator with components $e^{i\mathbf{k}\cdot\mathbf{c}_i}\delta_{ij}/w_i$ [note that $\mathbf{D}(0)=\mathbf{I}$]. The eigenvalues of $\mathbf{H}(\mathbf{k})$ defined from

$$\mathbf{H}(\mathbf{k})\circ\mathbf{e}_n(\mathbf{k})=e^{z_n(\mathbf{k})}\mathbf{e}_n(\mathbf{k}) \tag{15}$$

then give information about the transport coefficients corresponding to the collision matrix $\mathbf{C}$.

In the long-wavelength regime ($k\to 0$, where $k=|\mathbf{k}|$), two types of modes exist: soft hydrodynamic modes, related to the conservation laws, with $\mathrm{Re}[z(\mathbf{k})]\sim O(k^2)$, and hard rapidly decaying kinetic modes, with $\mathrm{Re}[z(\mathbf{k})]=O(1)<0$, without any physical significance. The transport coefficients are related to the hydrodynamic modes [16]. In a model without explicit energy conservation $d+1$ such hydrodynamic modes exist: two propagating but damped sound modes (denoted $\pm$) and $d-1$ diffusive transverse shear modes (denoted $\perp$). The real part of $z(\mathbf{k})$ represents damping and, if the imaginary part $\mathrm{Im}[z(\mathbf{k})]=\pm c_s(\mathbf{k})k$ is nonvanishing, the mode propagates with speed $c_s(\mathbf{k})$ [16]. In the limit $\mathbf{k}=\mathbf{0}$ the hydrodynamic modes correspond to the density and momentum eigenvectors of $\mathbf{C}$ and the other rapidly decaying modes correspond to the stress and ghost eigenvectors of $\mathbf{C}$.

A wave-vector-dependent kinematic shear viscosity [16] is defined for each shear mode as $\nu(\mathbf{k})=-z_\perp(\mathbf{k})/k^2$, while a sound velocity and a sound damping constant is defined for the sound modes as $c_s(\mathbf{k})=-\mathrm{Im}[z_\pm(\mathbf{k})/k]$ and $\Gamma(\mathbf{k})=-\mathrm{Re}[z_\pm(\mathbf{k})/k^2]$, respectively. In classical hydrodynamics, the transport coefficients are $\mathbf{k}$ independent by definition. However, when this situation does not hold, but the hydrodynamic modes are still clearly separated from the kinetic modes, one can speak of a *generalized hydrodynamic* regime [16], with transport coefficients which are slowly varying functions of $\mathbf{k}$. In lattice-based models, the transport coefficients might also depend on the direction of the wave vector, reflecting anisotropies due to the symmetry of the lattice. By computing the transport coefficients through the spectral analysis of the evolution operator and looking at their $\mathbf{k}$ dependence, one can judge the range of validity of the classical and the generalized hydrodynamic regime. In a previous analysis [16], for the simplest lattice gas Frisch-Hasslacher-Pomeau (FHP-I) model with a density of $\rho=1.8$, generalized hydrodynamics were shown to be val-

id up to $k \simeq 0.4$ for certain directions of $\mathbf{k}$ (Fig. 3 of Ref. [16]).

IV. RESULTS FOR GENERAL MODELS

We have done an extensive analysis of the hydrodynamic behavior of the models detailed in the Appendix for various values of the parameters and in various directions in $\mathbf{k}$ space. We summarize our results in this section and give representative plots of $-\mathrm{Re}[z(\mathbf{k})/k^2]$ and $-\mathrm{Im}[z(\mathbf{k})/k]$, which indicate the hydrodynamic behavior as discussed above. We will display results principally for the D3Q14 model since this is the more

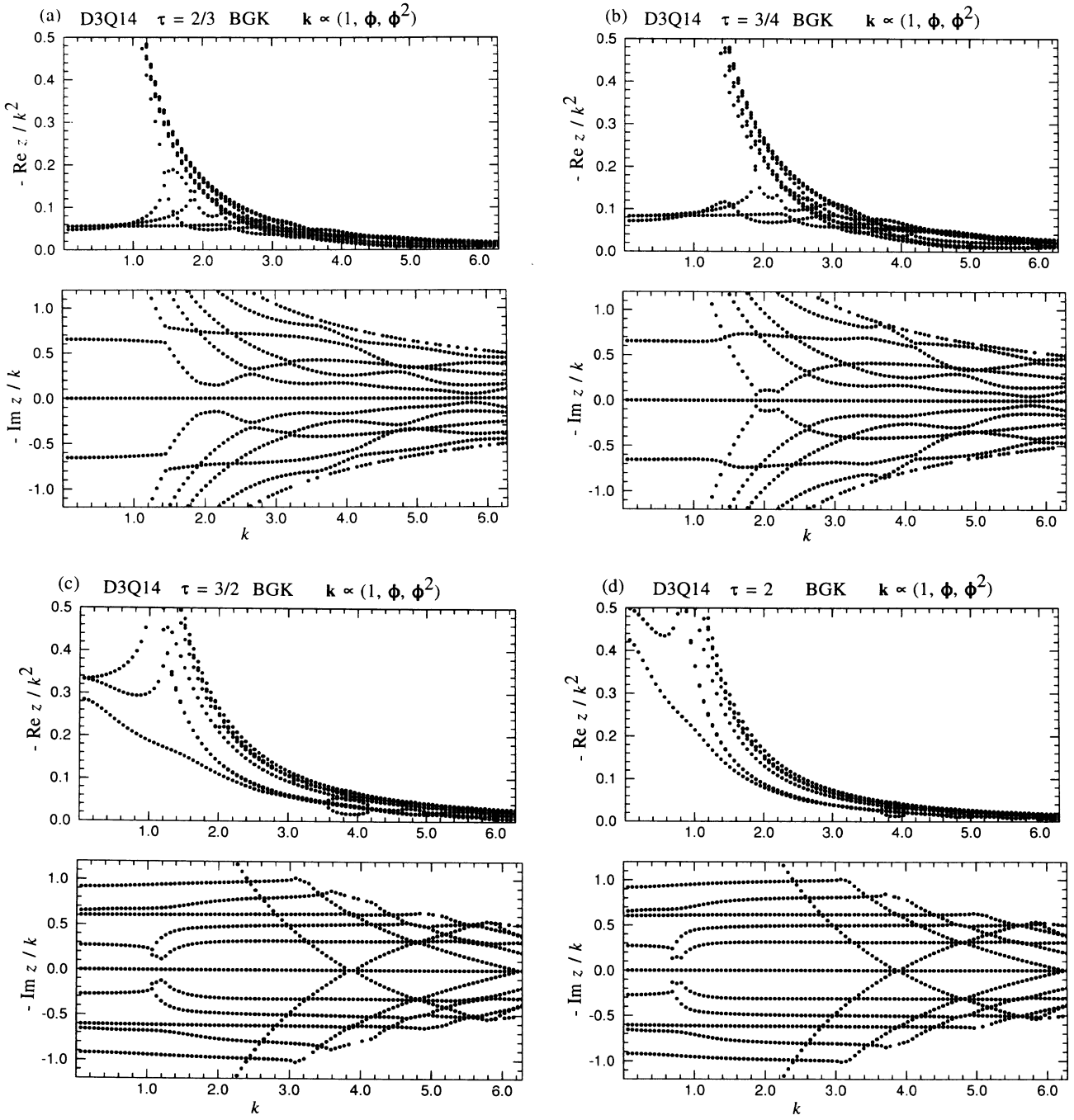

FIG. 1. Hydrodynamic behavior of the D3Q14 BGK model along an arbitrarily chosen direction $\mathbf{k} \propto (1, \phi, \phi^2)$ [$\phi = (1+\sqrt{5})/2$] for several values of the relaxation time parameter τ. Plots (a), (b), (c), and (d) are for $\tau = \frac{2}{3}, \frac{3}{4}, \frac{3}{2}$, and 2, respectively. For each value of τ the upper plot shows $-\mathrm{Re}z(\mathbf{k})/k^2$ against k and the lower plot $-\mathrm{Im}z(\mathbf{k})/k$ against k, for all eigenmodes determined by Eq. (15) in the main text. The soft hydrodynamic modes have $\mathrm{Re}z = O(k^2)$ and $\mathrm{Im}z = O(k)$ or 0 as $k = |\mathbf{k}| \to 0$. On these plots such modes appear as horizontal lines as $k \to 0$; deviations from constant behavior indicate the limits of validity of classical hydrodynamics in the LB fluid. The hard, kinetic modes start to appear on these plots for larger k and they limit the range of validity of generalized hydrodynamics.

efficient method for three-dimensional simulations. The hydrodynamic behavior of other models follows qualitatively the same trends.

Figure 1 shows the hydrodynamic behavior of the D3Q14 BGK model for $\mathbf{k}$ in an arbitrary chosen, fixed direction $(1,\phi,\phi^2)$ [ϕ being the golden mean $(1+\sqrt{5})/2 \approx 1.618$], for four values of the relaxation parameter τ. Clearly relatively good hydrodynamic behavior is achieved for $\tau < 1$, whereas very poor hydrodynamic behavior is seen for $\tau > 1$. The behavior at $\tau = 1$ is a special case and will be discussed in Sec. V. The trend of improved hydrodynamic behavior as τ decreases past unity is reflected in all the models.

For the $\tau = \frac{3}{4}$ D3Q14 model Fig. 2 shows the behavior in various directions in $\mathbf{k}$ space. There is some dependence on direction and one particular point to note is that $z \to 0$ at some isolated points $\mathbf{k} \neq 0$, for example, $\mathbf{k} = (\pi,0,0)$ in Fig. 2. These are the *staggered momentum* modes and correspond to spurious conservation laws [16]. They are artificial effects due to the lattice and are present in all models.

Hydrodynamics for the generalized BGK model with $\lambda = -\frac{4}{3}$ and $\sigma = -1$ is shown in Fig. 3. The hydrodynamic behavior has been further improved when com-

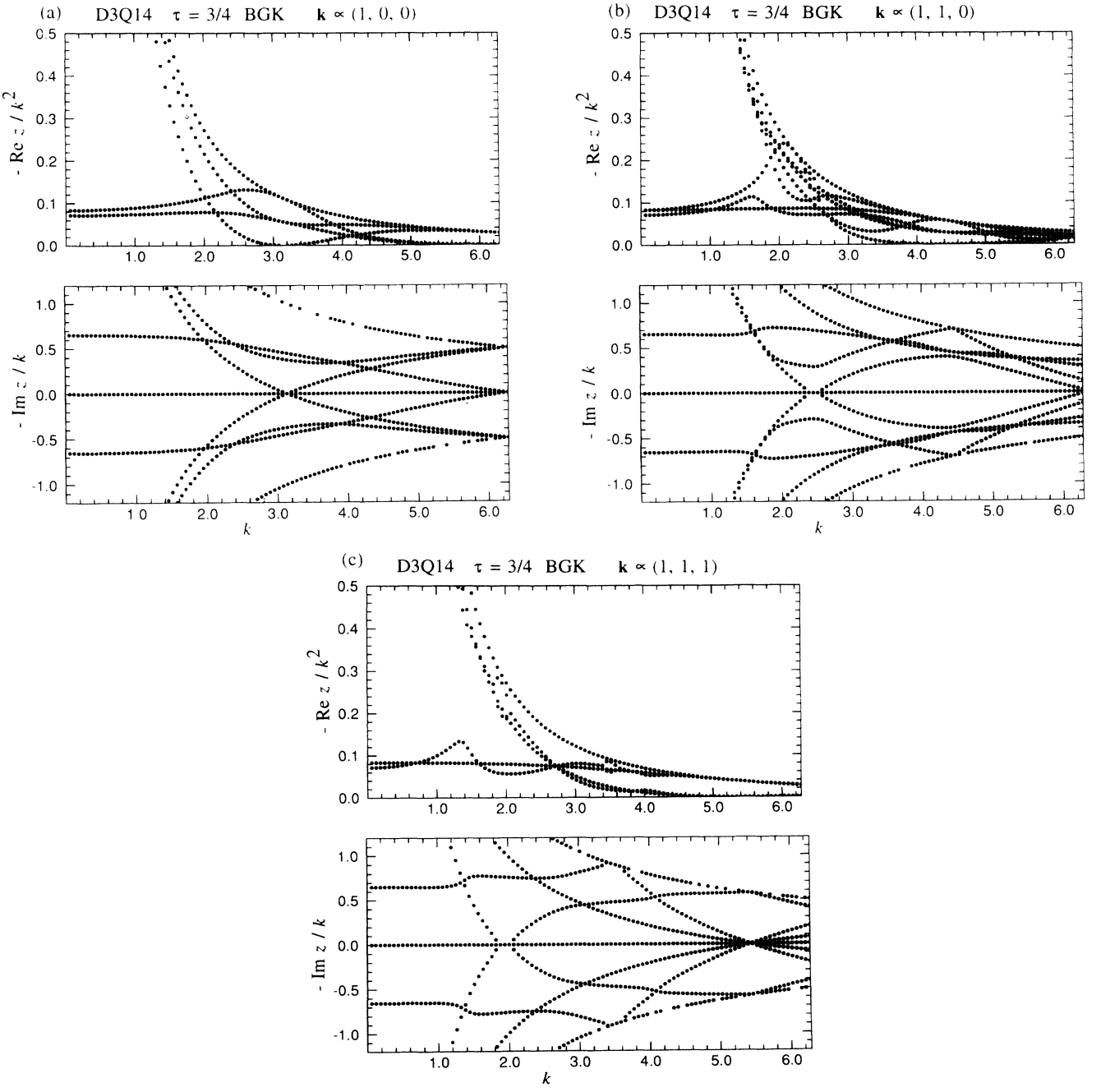

FIG. 2. Hydrodynamic behavior of the D3Q14 $\tau = \frac{3}{4}$ BGK model along various directions in $\mathbf{k}$ space. Plots (a), (b), and (c) are for $\mathbf{k} \propto (1,0,0)$, $(1,1,0)$, and $(1,1,1)$, respectively. For the behavior for $\mathbf{k} \propto (1,\phi,\phi^2)$ see Fig. 1(b).

pared with the previous $\tau=\frac{3}{4}$ BGK model for which $\lambda=\sigma=-\frac{4}{3}$. An extensive range of classical hydrodynamics is obtained: almost constant transport coefficients are obtained up to $k\approx 2.0$ in all directions in **k** space.

Finally, in Fig. 4 we look at the effect of adding rest particles, on the D2Q7 $\tau=\frac{3}{4}$ BGK models for a change. The range of classical hydrodynamics and generalized hydrodynamics is not greatly affected by the change. The speed of sound is reduced on increasing the weight in the rest particle state and the sound dissipation constant is increased towards the kinematic viscosity.

V. $\tau=1$ BGK MODEL

The BGK model with unit relaxation time $\tau=1$ deserves special attention because computationally it is a very efficient algorithm:

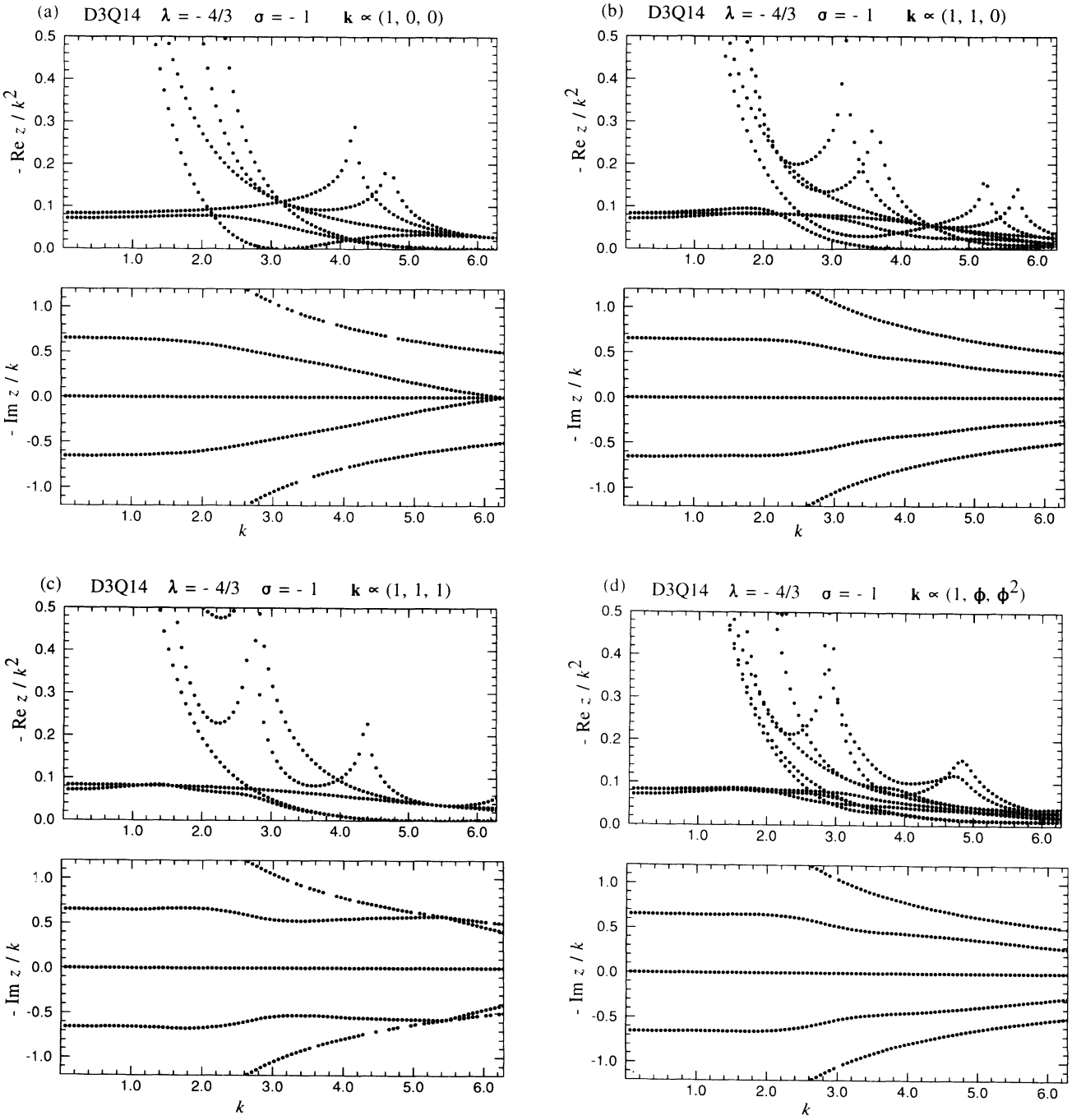

FIG. 3. Hydrodynamic behavior of the D3Q14 generalized BGK model with parameters $\lambda=-\frac{4}{3}$ and $\sigma=-1$ (see main text for definition of this model), along various directions in **k** space. Plots (a), (b), (c), and (d) are for $\mathbf{k}\propto(1,0,0)$, $(1,1,0)$, and $(1,1,1)$, and $(1,\phi,\phi^2)$, respectively.

$$f_i(\mathbf{r}+\mathbf{c}_i,t+1)=f_i^{(\mathrm{eq})}(\mathbf{r},t)\ . \tag{16}$$

Setting $\tau=1$ in the equations in the previous sections gives $\mathbf{C}^R=-\mathbf{P}^{SG}$ and $\mathbf{H}(\mathbf{k})=\mathbf{D}(\mathbf{k})\cdot\mathbf{P}^{\rho\mathbf{J}}$. Clearly $\mathbf{A}^S$ and $\mathbf{A}^G$ are eigenvectors of this operator for all $\mathbf{k}$, possessing the eigenvalue zero, because $\mathbf{H}$ is just the operator $\mathbf{D}(\mathbf{k})$ right projected onto the space spanned by $\mathbf{A}^\rho$ and $\mathbf{A}^\mathbf{J}$. It also follows that the eigenvectors of $\mathbf{H}(\mathbf{k})$ with generally nonzero eigenvalues are only found in this subspace. By projecting $\mathbf{H}(\mathbf{k})$ onto $\mathbf{A}^\rho$ and $\mathbf{A}^\mathbf{J}$ (which form an orthonormal basis) one can construct a $(d+1)\times(d+1)$ matrix $\tilde{\mathbf{H}}(\mathbf{k})$, which possesses the same eigenvalues as $\mathbf{H}(\mathbf{k})$ apart from the trivial, identically zero ones belonging to the stress and ghost mode eigenvectors. It is not too difficult to show that this new matrix is

$$\tilde{\mathbf{H}}=\begin{pmatrix} 1/b\sum_i w_i e^{i\mathbf{k}\cdot\mathbf{c}_i} & \sqrt{D/b^2c^2}\sum_i w_i e^{i\mathbf{k}\cdot\mathbf{c}_i}c_{i\beta} \\ \sqrt{D/b^2c^2}\sum_i w_i e^{i\mathbf{k}\cdot\mathbf{c}_i}c_{i\alpha} & D/bc^2\sum_i w_i e^{i\mathbf{k}\cdot\mathbf{c}_i}c_{i\alpha}c_{i\beta} \end{pmatrix}. \tag{17}$$

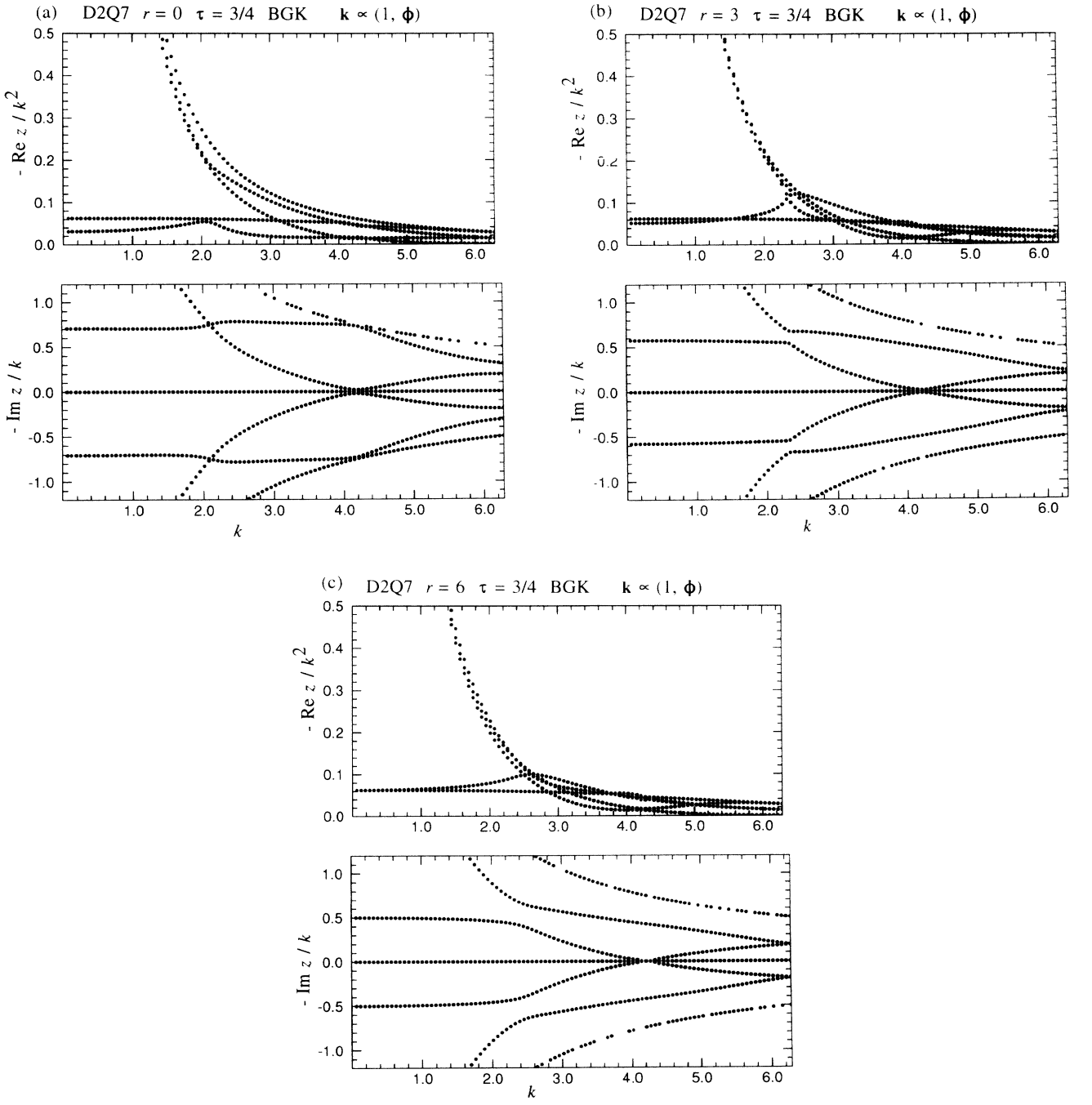

FIG. 4. The effect of changing weight r in the rest particle state on the hydrodynamic behavior of the D2Q7 $\tau=\frac{3}{4}$ BGK model, along an arbitrarily chosen direction $\mathbf{k}\propto(1,\phi)$. Plots (a), (b), and (c) are for $r=0$, 3, and 6, respectively.

An expansion in $\mathbf{k}$ may be made and the eigenvalues and the eigenvectors extracted after some tedious algebra, making use of Eqs. (2). They are, for $k \to 0$ (where $k = |\mathbf{k}|$),

$$z_{\perp} = -\frac{c^2}{2(D+2)}k^2 + \cdots \quad (d-1)\text{-fold degenerate}$$
$$z_{\pm} = \pm ik\left[\frac{c^2}{D}\right]^{1/2} - \frac{c^2(D-1)}{2D(D+2)}k^2 + \cdots . \tag{18}$$

Thus we identify the kinematic viscosity $\nu = c^2/2(D+2)$, the speed of sound $c_s = \sqrt{(c^2/D)}$, and the sound damping constant $\Gamma = c^2(D-1)/2D(D+2)$. The kinematic viscosity is in agreement with Eq. (13) and the speed of sound is also as expected.

Figure 5 shows plots of $-\mathrm{Re}[z(\mathbf{k})/k^2]$ and $-\mathrm{Im}[z(\mathbf{k})/k]$ for various directions in $\mathbf{k}$ space. While the calculation above gives the behavior as $k \to 0$, the plots reveal some interesting behavior at nonzero $\mathbf{k}$ values. There are divergences in the behavior at some

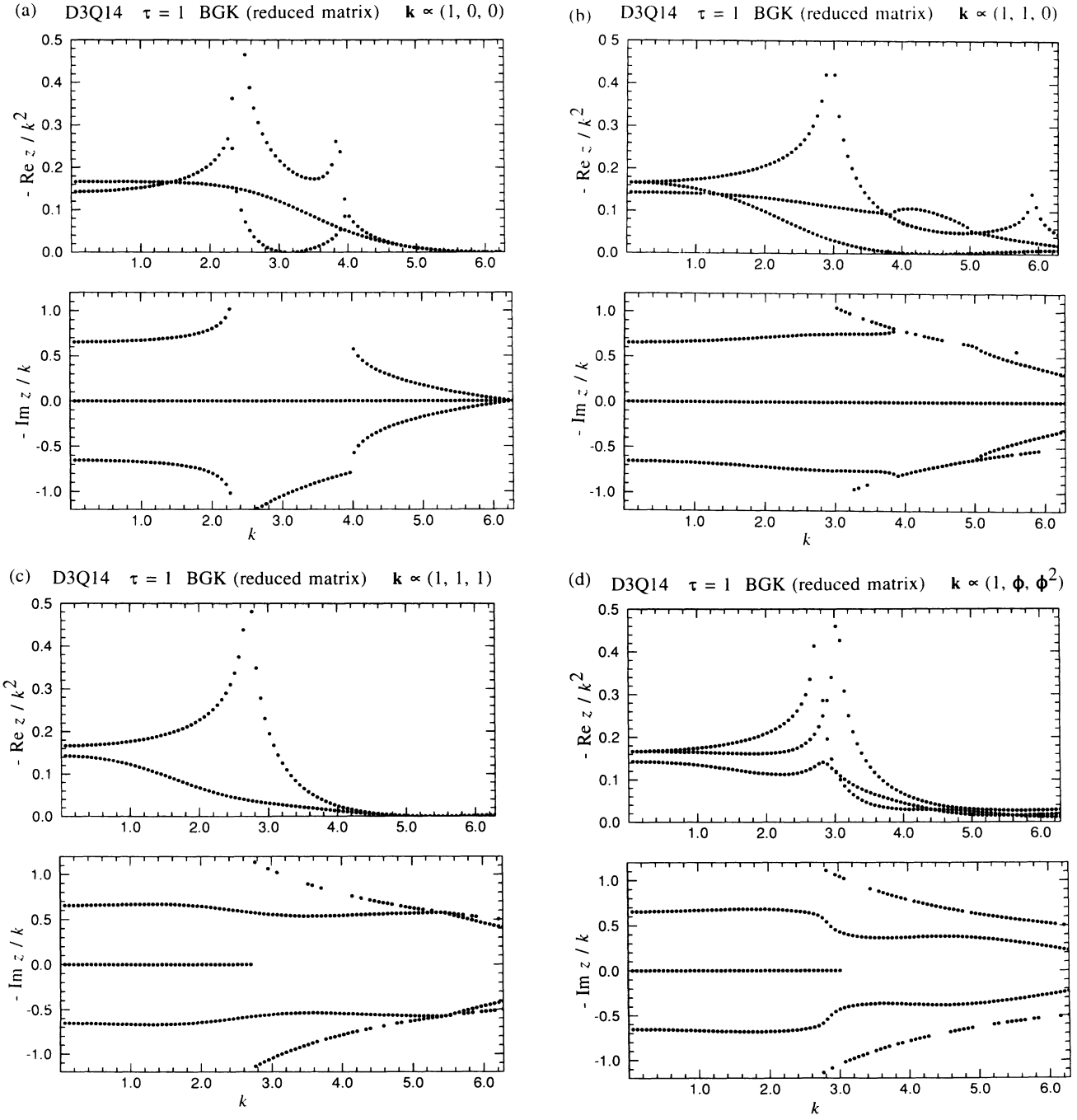

FIG. 5. Hydrodynamic behavior of the D3Q14 $\tau = 1$ BGK model as determined from the reduced matrix $\tilde{\mathbf{H}}$, defined in Eq. (17) in the main text. Plots (a), (b), (c), and (d) are for $\mathbf{k} \propto (1,0,0)$, $(1,1,0)$, $(1,1,1)$, and $(1,\phi,\phi^2)$, respectively.

places in $\mathbf{k}$ space, for example, at $\mathbf{k}=(\pi-\cos^{-1}\frac{3}{4},0,0)$, which can be traced to zero eigenvalues of the matrix $\tilde{H}$ (i.e., $z\to-\infty$ or $e^z\to 0$ at these $\mathbf{k}$ values). Such divergences distort the hydrodynamic behavior, which, consequently, is not as good as that seen for the $\tau<1$ models.

VI. CONCLUSION AND DISCUSSION

The trends found in the preceding section are very clear. BGK models with $\tau>1$ have a very poor range of classical and generalized hydrodynamics. Much better ranges of validity are found in models with $\tau<1$. Also the $\tau=1$ BGK model, while being a simple algorithm to implement, does not have a particularly wide range of classical hydrodynamic behavior. These trends were common to all the models studied.

At the price of a slight increase in complexity, even better ranges for classical and generalized hydrodynamics can be achieved for the two-parameter BGK models, again provided the appropriate stress relaxation time $-1/\lambda<1$. The additional ghost relaxation time $-1/\sigma$ may conveniently be set to unity. Thus for the model shown in Fig. 3, near classical hydrodynamics holds for $k\approx 2.0$, in all directions in $\mathbf{k}$ space. The increased complexity lies in the construction of the collision matrix, which is defined in Eq. (12). However, such a step only has to be performed once in the initialization of a LB simulation and the net computational cost is fairly slight.

The biggest computational cost in reducing the relaxation time τ is the corresponding reduction in kinematic viscosity. The time taken for the fluid to reach a steady state in a simulation box of size L is of order L^2/ν; thus a reduction in ν inevitably means an increase in this time. This is of significance in the simulation of colloidal suspensions, for instance, where a separation of time scales between the dynamics of the fluid and the dynamics of colloid particle relaxation must be maintained.

Finally we note that there are valid hydrodynamic solutions to the LB kinetic equation (1) that cannot be constructed out of the type of solutions we have been discussing up to now [22]. For example,

$$f_i(\mathbf{r})=\frac{\rho}{b}+\frac{\rho D}{bc^2}E_{\alpha\beta}c_{i\alpha}(r_\beta+c_{i\beta}/\lambda)\ , \tag{19}$$

where λ is again the stress mode eigenvalue, represents a uniform shearing flow with

$$u_\alpha=\frac{J_\alpha}{\rho}=E_{\alpha\beta}r_\beta\ . \tag{20}$$

It is readily checked that (19) solves (1) independent of the model. This type of solution cannot be constructed in a periodic box and requires boundary conditions such as moving walls to maintain it; thus it is missed by the Fourier transform which underlies the $\mathbf{k}$-dependent wave-vector analysis we have been discussing. Its existence indicates that the rich hydrodynamic behavior of the LB equation is not completely revealed even by full wave-vector analysis.

ACKNOWLEDGMENTS

O.B. acknowledges financial support through a Foreign Office-Glaxo joint scholarship. R.H. acknowledges financial support from the NSERC of Canada and le Fonds pour la Formation des Chercheurs et l'Aide à la Recherche de la Province du Québec.

APPENDIX

We give below details of four common models. Again we use the notation of Qian, d'Humières, and Lallemand [9], in which DdQn denotes an n-link model on a d-dimensional lattice. Link weights and directions are w_i and $\mathbf{c}_i$ and associated parameters are b, D, and c^2. In terms of an underlying LGA, these parameters can be interpreted as the number of particles per node, an effective dimension, and the square of the particle velocity, but in general they must be regarded as being determined by Eqs. (2) in the main text. The speed of sound in all the models is given by $c_s^2=\sqrt{(c^2/D)}$, but specification of kinematic viscosity requires the stress mode eigenvalue λ and is given by Eq. (13) in the main text.

D2Q6 is a two-dimensional model on a triangular lattice with six inks per node to the nearest neighbors $\mathbf{c}_i=(\pm 1,0),(\pm\frac{1}{2},\pm\sqrt{3}/2)$ with $w_i=1$. The parameters are $b=6$, $D=2$, and $c^2=1$.

D2Q8 is a two-dimensional model on a square lattice with four links per node to the nearest neighbors $\mathbf{c}_i=(\pm 1,0),(0,\pm 1)$ with $w_i=4$ and four links per node to the next-nearest neighbors $\mathbf{c}_i=(\pm 1,\pm 1)$ with $w_i=1$. The parameters are $b=20$, $D=\frac{5}{2}$, and $c^2=\frac{3}{2}$.

D3Q14 is a three-dimensional model on a simple cubic lattice with six links per node to the nearest neighbors $\mathbf{c}_i=(\pm 1,0,0),(0,\pm 1,0),(0,0,\pm 1)$ with $w_i=8$ and eight links per node to the next-next-nearest neighbors $\mathbf{c}_i=(\pm 1,\pm 1,\pm 1)$ with $w_i=1$. The parameters are $b=56$, $D=7$, and $c^2=3$.

D3Q18 is another three-dimensional model on a simple cubic lattice with six links per node to the nearest neighbors $\mathbf{c}_i=(\pm 1,0,0),(0,\pm 1,0),(0,0,\pm 1)$ with $w_i=2$ and twelve links per node to the next-nearest neighbors $\mathbf{c}_i=(\pm 1,\pm 1,0),(\pm 1,0,\pm 1),(0,\pm 1,\pm 1)$ with $w_i=1$. The parameters are $b=24$, $D=4$, and $c^2=2$.

In these models one may also include a rest particle state, with $\mathbf{c}_i=0$, in which case the model becomes a DdQ$(n+1)$ model. The weight in the rest particle state must also be given to fully determine the model: The parameters b, D, and c^2 may again be determined from Eqs. (2). Adding a rest particle state of weight r to the models above we obtain $b=6+r$, $D=2(6+r)/(6-r)$, and $c^2=6/(6-r)$ for D2Q7; $b=20+r$, $D=2(20+r)/(16-r)$, and $c^2=24/(16-r)$ for D2Q9; $b=56+r$, $D=2(56+r)/(16-r)$, and $c^2=48/(16-r)$ for D3Q15; and $b=24+r$, $D=2(24+r)/(12-r)$, and $c^2=24/(12-r)$ for D3Q19.

In terms of models already considered in the literature, D2Q6 clearly derives from the original FHP-I LGA [1] and D3Q18 derives from the three-dimensional projection of the four-dimensional face centered hypercubic LGA [2]. Although D3Q14 is suggestive of a seven-

dimensional LGA (since $D=7$), we have been unable to construct one that projects down to the particular set of link vectors and weights in this model. If the rest particle state in D3Q15 has weight $r=8$, we obtain a model used by Alexander, Chen, and Grunau [23] with $b=64$, $D=16$, and $c^2=16$. By setting $r=16$ in D3Q15 we obtain one of the models considered by Qian, d'Humières, and Lallemand [9] for which $b=72$ and $c^2/D=c^2/(D+2)=\frac{1}{3}$ (no solution can be obtained for D and c^2 separately unless one allows formally $D,c^2\to\infty$ with D/c^2 fixed at 3).

The three-dimensional models can be projected down to two-dimensional models simply by ignoring the value of c_{iz} and combining those links with the same (c_{ix},c_{iy}). Thus D3Q14 and D3Q18 both project down to D2Q9 with $r=8$ and 4, respectively (a common factor may be divided out of the weights for the D3Q14 projection). The values of b, c^2, and D are unchanged in such a projection and the hydrodynamic behavior is simply given by the $k_z=0$ hydrodynamics of the original versions, although some of the hard kinetic modes will be lost.

[1] U. Frisch, B. Hasslacher, and Y. Pomeau, Phys. Rev. Lett. **56**, 1505 (1986).

[2] D. d'Humières, P. Lallemand, and U. Frisch, Europhys. Lett. **2**, 291 (1986).

[3] U. Frisch, D. d'Humières, B. Hasslacher, P. Lallemand, Y. Pomeau, and J.-P. Rivet, Complex Syst. **1**, 649 (1987) [reprinted in *Lattice Gas Methods for Partial Differential Equations*, edited by G. Doolen (Addison-Wesley, Singapore, 1990)].

[4] G. R. McNamara and G. Zanetti, Phys. Rev. Lett. **61**, 2332 (1988).

[5] F. J. Higuera, S. Succi, and R. Benzi, Europhys. Lett. **9**, 345 (1989).

[6] F. J. Higuera and J. Jiménez, Europhys. Lett. **9**, 663 (1989).

[7] P. Bhatnagar, E. P. Gross, and M. K. Krook, Phys. Rev. **94**, 511 (1954).

[8] S. Chen, H. Chen, D. Matinez, and W. Matthaeus, Phys. Rev. Lett. **67**, 3776 (1991).

[9] Y. H. Qian, D. d'Humières, and P. Lallemand, Europhys. Lett. **17**, 479 (1992).

[10] H. Chen, S. Chen, and W. Matthaeus, Phys. Rev. A **45**, R5339 (1992).

[11] S. Chen, Z. Wang, X. Shan, and G. D. Doolen, J. Stat. Phys. **68**, 379 (1992).

[12] M. Vergassola, R. Benzi, and S. Succi, Europhys. Lett. **13**, 411 (1990).

[13] R. Benzi, S. Succi, and M. Vergassola, Phys. Rep. **222**, 147 (1993).

[14] A. K. Gunstensen, D. H. Rothman, S. Zaleski, and G. Zanetti, Phys. Rev. A **43**, 4320 (1991).

[15] A. J. C. Ladd, Phys. Rev. Lett. **70**, 1339 (1993).

[16] S. P. Das, H. J. Bussemaker, and M. H. Ernst, Phys. Rev. E **48**, 245 (1993).

[17] See, for example, P. Resibois and M. de Leener, *Classical Kinetic Theory of Fluids* (Wiley, New York, 1977).

[18] L.-S. Luo, H. Chen, S. Chen, G. D. Doolen, and Y.-C. Lee, Phys. Rev. A **43**, 7097 (1991).

[19] P. Grosfils, J.-P. Boon, R. Brito, and M. H. Ernst, Phys. Rev. E **48**, 2655 (1993).

[20] D. d'Humières and P. Lallemand, Complex Syst. **1**, 599 (1987).

[21] The D2Q6 model has only two independent components of $Q_{i\alpha\beta}$, not three, since $Q_{ixx}=-Q_{iyy}$. This deficiency can be cured by introducing a rest particle state.

[22] M. Hénon, Complex Syst. **1**, 763 (1987).

[23] F. J. Alexander, S. Chen, and D. W. Grunau, Phys. Rev. B **48**, 634 (1993).